Eur. Phys. J. D **1**, 271–276 (1998)

THE EUROPEAN PHYSICAL JOURNAL D

Collision induced dissociation of the heteronuclear alkali ion NaK^+. Comparison with the Na_2^+ and K_2^+ dissociations

M. Barat[a], J.C. Brenot, H. Dunet, J.A. Fayeton, and Y.J. Picard

Laboratoire des Collisions Atomiques et Moléculaires[b], Université Paris-Sud, 91405 Orsay Cedex, France

Received: 3 October 1997 / Revised: 1 December 1997 / Accepted: 16 January 1998

Abstract. An experimental study of the dissociation of the heteronuclear NaK^+ ion by collisions with He and H_2 targets at a collision energy of 2.4 keV is presented. The use of a technique based on the measurement of the velocity vectors of the fragments allows investigating in detail the two basic dissociation mechanisms: impulsive and electronic. In the present asymmetric case, one is able to assess the relative role of close encounters with each of the Na^+ and K^+ atomic cores of the molecule. Electronic transitions at a surface crossing are proposed to explain processes which happens in close collisions between the K^+ core and the He target.

PACS. 34.50.-s Scattering of atoms, molecules, and ions – 34.50.Pi State-to-state scattering analyses – 36.40.Qv Stability and fragmentation of clusters

1 Introduction

In a recent experiment, a new technique that allows a complete analysis of the dissociation of diatomic molecular [1,2] and cluster [3] ions at keV collision energies has been presented. This experiment put in evidence a competition between two basic dissociation mechanisms: *(i) the impulsive mechanism* (IM) in which the dissociation is due to a momentum transfer in a close encounter between the target atom and one atomic core, the "hit" atom, of the molecule, *(ii) the electronic mechanism* (EM) in which the molecule is brought into a dissociative electronically excited state. In the present paper we extend this analysis, initially carried out with Na_2^+ ions, to the heteronuclear NaK^+ ions. A comparison with the results obtained for the homonuclear Na_2^+ and K_2^+ ions brings new insight into the dissociation mechanisms.

The experimental technique described in detail in [2] is essentially based on the simultaneous measurement of the velocity vectors of the two fragments. Alkali molecules produced in a oven heated at 650 °C are ionised by 50 eV electrons. The molecular ions thus produced are accelerated at a collision energy of 2.4 keV and are mass selected before crossing a "cold" He or H_2 target beam produced by a supersonic expansion. The charged and neutral fragments are separated in an electrostatic analyser. The neutral fragments fly in a straight line towards a first two-dimension position sensitive detector (PSD), while the electric field bends the trajectories of the ionic fragments. Neutral and ionic fragments are detected in coincidence using a second PSD. In the present experiment one can then separately investigate the $K^+ + Na$ and $K + Na^+$ dissociation channels by tuning the electric field of the analyser in order to detect either the Na^+ or the K^+ fragment. In the complete analysis of the kinematics of the collision one must choose the most significant correlation between the various parameters [2]. Three types of correlation maps are used below. They represent (see bottom of Fig. 1) as a function of χ the centre-of-mass (CM) scattering angle, the relative kinetic energy $E_{\rm rel}$ of the two fragments, the angle ϕ between the dissociation and the collision planes and the angle α between the incident beam and the internuclear axis of the molecule.

2 The $K^+ + Na$ channels

The $\phi(\chi)$ correlation maps (Fig. 1) readily show that the dissociation occurs primarily at large χ angles and takes place in (or close to) the collision plane, at $\phi = 0°$ and $\phi = 180°$ for both K_2^+ and NaK^+ dissociation. This behaviour corresponds to impulsive dissociation (IM) in the $^2\Sigma$ ground state (Fig. 2). For $NaK^+ \rightarrow Na + K^+$, $\phi = 0°$ corresponds to the case when the Na^+ core is hit resulting in a Na atom scattered at a large angle, whereas the peak at $\phi = 180°$ is for the K^+ core being hit and side scattered. One notices in Figure 1, that in both $K^+ + K$ and $K^+ + Na$ contour maps, the same structures appear at $\phi = 180°$ when the K^+ core is side scattered. This feature reflects the binary K^+ He collision that is common to both systems. Filtering the raw NaK^+ data around these two ϕ values, $-90° < \phi < 90°$ and $90° < \phi < 270°$, provides

[a] e-mail: barat@lcam.u-psud.fr
[b] URA CNRS D 0281

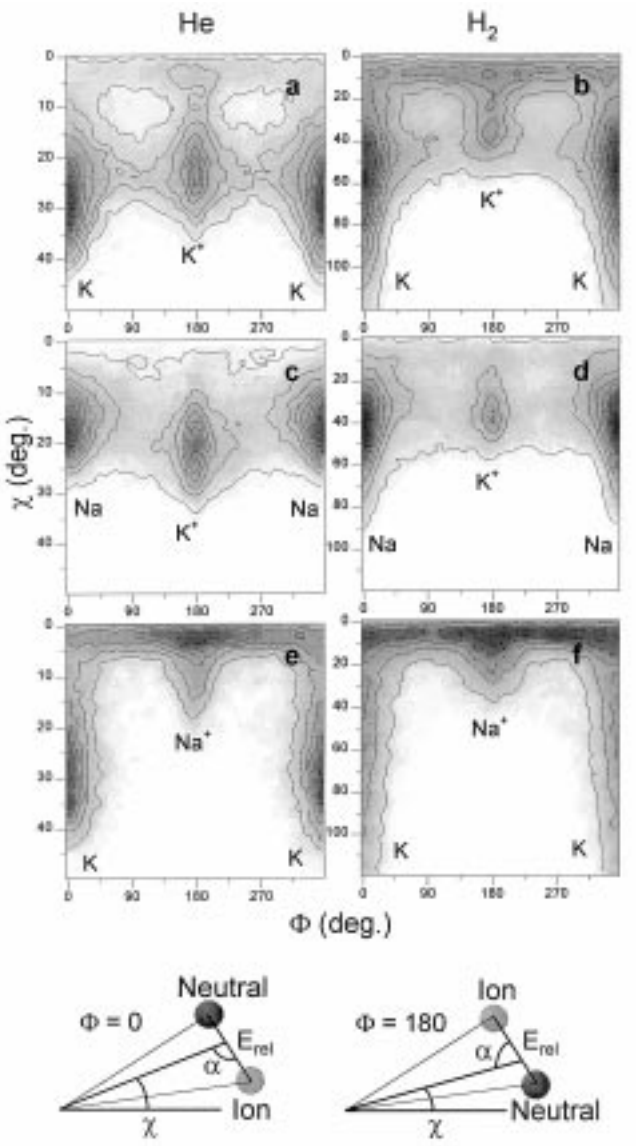

Fig. 1. $\phi(\chi)$ contour maps for dissociation of K_2^+ and NaK^+ on He and H_2 targets in linear scale: (a,b): K_2^+, (c,d): $NaK^+ \rightarrow K^+ + Na$, (e,f): $NaK^+ \rightarrow K + Na^+$. The origin $\phi = 0°$ was arbitrarily chosen when the hit core becomes the neutral fragment (the scattered fragment is indicated); bottom: schematic view of the dissociation geometry and definitions of the various angles (see text).

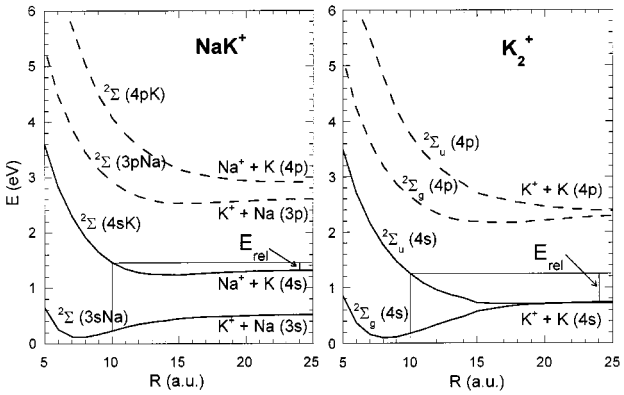

Fig. 2. The lowest $^2\Sigma$ potential energy curves of NaK^+ and K_2^+ taken from [4]. Also schematically shown the relative kinetic energy $E_{\rm rel}$ of the fragments given by a transition to the first $^2\Sigma$ excited state.

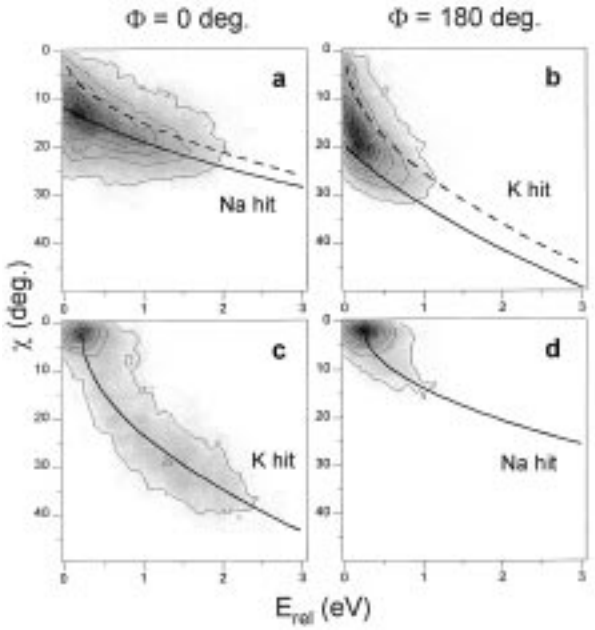

Fig. 3. Filtered $E_{\rm rel}(\chi)$ contour maps, in linear scale, for NaK^+ colliding with He target at $\phi = 0°$ and $\phi = 180°$. (a,b): $K^+ + Na$ channel, (c,d): $K + Na^+$ channel. The predictions of the binary model are also shown. *Full lines*: the ion is in the rovibrational ground state, *dashed lines*: the ion is rovibrationally excited at the dissociation limit. The dissociation energy of NaK^+ is taken from [5].

a way to select one of the two situations: a collision with the Na^+ or with the K^+ core.

The filtered $E_{\rm rel}(\chi)$ contours, only shown for He in Figure 3a,b, follow well the curves given by a simple kinematic model [1,2]. This model assumes an elastic binary momentum transfer between one atom of the molecule and the target ignoring the second atom of the molecule. The energy $E_{\rm rel}$ of the fragments and the χ angle are then given by equations (1) and (2):

$$E_{\rm rel} = \frac{4\mu {M_{\rm T}}^2 E_0 \sin^2 \frac{\chi_1}{2}}{(M_{\rm T} + M_{\rm A})^2 M_{\rm AB}} - E_{\rm diss} \qquad (1)$$

$$\tan\chi = \frac{\sin\chi_1}{\cos\chi_1 + \frac{(M_{\rm AB} - M_{\rm A})M_{\rm T}}{(M_{\rm AB} + M_{\rm T})M_{\rm A}}} \qquad (2)$$

where $M_{\rm T}$, $M_{\rm A}$, $M_{\rm AB}$ and μ are: the target mass, the hit atom mass, the dimer mass and the dimer reduced mass respectively. The χ_1 angle is the target-hit core scattering angle. E_0 is the projectile energy and $E_{\rm diss}$ the dissociation energy of the dimer, which depends of the unknown initial internal energy of the molecular ion. The model is therefore given for two limiting cases: the lowest and the highest possible rovibrational states respectively.

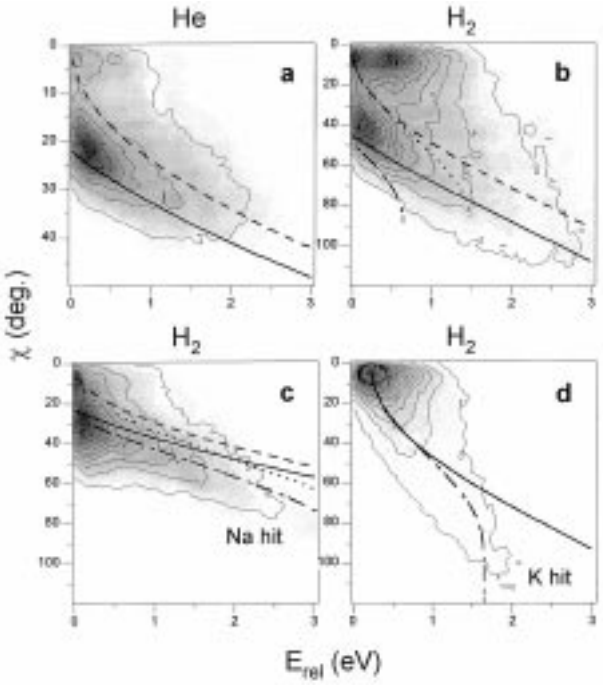

Fig. 4. Unfiltered $E_{\rm rel}(\chi)$ contour maps in linear scale for dissociation of (a) K_2^+ on He, (b) K_2^+ on H_2, (c) $NaK^+ \rightarrow K^+ + Na$ and (d) $NaK^+ \rightarrow K + Na^+$ on H_2. The predictions of the binary model are also shown. For K_2^+ on He, same labels as in Figure 3. For NaK^+ and K_2^+ on H_2, two sets of curves are drawn considering binary collisions with the Na^+ and K^+ core respectively. *full* and *dashed lines*: considering a binary collision of K and Na respectively with a target of mass 2 (H_2-model). *Dashed-dotted and dotted lines*: as before but for a binary collision with a single H atom (H-model).

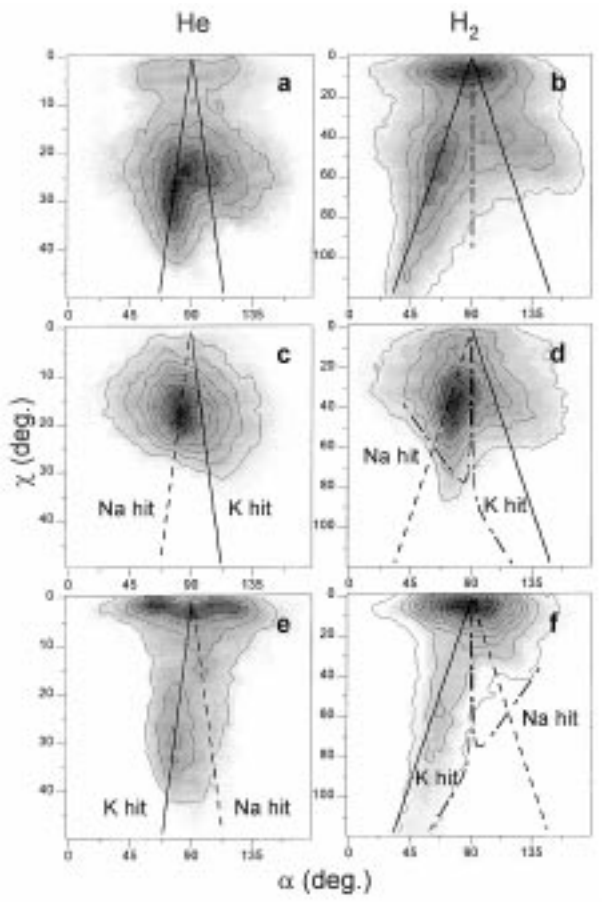

Fig. 5. $\alpha(\chi)$ contour maps in linear scale (same labels as in Fig. 1). The predictions of the binary model are also shown. For the He target, *full* and *dashed lines*: the K and Na cores are scattered respectively. For H_2 target, *full* and *dashed lines*: as for the He target, considering a binary collision with a target of mass 2. *Dashed-dotted lines*: as before but for a binary collision with a single H atom.

Considering the H_2 target (Fig. 4c), two models have been considered: a binary collision with one H atom, the H-model which has already been invoked to account for the $Na_2^+ - H_2$ results [2], and the H_2-model in which H_2 is considered as an atom of mass 2. In the H-model, $E_{\rm rel}$ is expressed by equation (1) in which $M_{\rm T} = M_{\rm H}$ the mass of the hydrogen atom and χ is given by:

$$\tan\chi = \frac{\sin\chi_1}{\cos\chi_1 + \dfrac{2(M_{\rm AB} - M_{\rm A})M_{\rm H} + M_{\rm A}M_{\rm AB}}{(M_{\rm AB} + 2M_{\rm H})M_{\rm A}}}\cdot \qquad (3)$$

Figure 5 shows the dependence of the cross section upon χ and α the orientation angle of the dissociation axis with respect to the scattering direction of the CM of the molecular ion. With He as a target, the contour lines for both K_2^+ and NaK^+ ions fall on the two lines characteristic of the impulsive model: $\alpha = \pi/2 \pm (\chi - \chi_1/2)$. With H_2 as a target, the results disagree with the prediction of the H-model and are better accounted for by the H_2-model. For collisions involving a heavy projectile and a light target, there is a maximum laboratory scattering angle determined by the mass ratio of the two partners of the collision. With the H-model applied to the dissociation of NaK^+, the kinematics lead to a limit angle of about 80° when the Na^+ core is hit. The double branch of the lines corresponds to a forward and a backward scattering in the CM frame.

The differential cross sections $d\Sigma/d\chi$ obtained by summing the data over $E_{\rm rel}$, are displayed on Figures 6c,d. They show, in addition to the impulsive contributions appearing at large χ, a minor contribution at small scattering angle. The latter contribution is attributed to a dissociation of an electronic excited state of NaK^+, most probably one leading to $K^+ + Na(3p)$. It is noteworthy that this contribution does not depend on the ϕ filtering, a feature which is consistent with the EM, since for this mechanism the target passes rather far from both cores. The integration of the $d\Sigma/d\chi$ cross sections over the scattering angle, allows to estimate the relative contributions of the various dissociation processes (Tab. 1). Notice that the contribution due to binary Na^+-target encounters is larger than that of K^+ ones. Actually their relative importance is governed by two opposite effects: the elastic scattering cross section increases while the momentum transfer decreases with the size of the ionic core

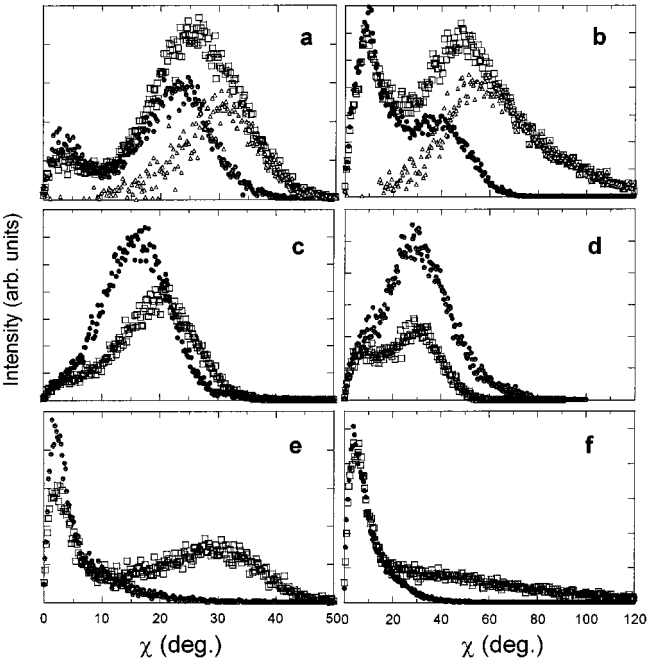

Fig. 6. Differential cross sections $d\Sigma/d\chi$ corresponding to the filtered data (same labels as in Fig. 1). Open squares: The K atom (a,b and e,f), or the K^+ ion (c,d) is side scattered. *Full circles*: The K^+ ion (a,b), the Na atom (c,d) or the Na^+ ion (e,f) is side scattered. In (a,b), the difference (*open triangles*) between the two contributions, tentatively attributed to the K(4p) excitation, is also shown.

that is hit. In fact the latter effect dominates. This may be seen in a simple way integrating, for each binary encounter, the elastic cross section from a threshold angle determined by the minimum momentum transfer for dissociation. The relevant potential used in these calculations is taken from [6] for the He-Na^+ interaction and is estimated using the "combining rule" [7] for the He-K^+ pair. The results of this simple calculation (K hit: 36%, Na hit: 49%) reproduce well the experimental values of the impulsive process (see Tab. 1).

3 The K + Na^+ channels

Contrary to the previous case, the $\phi(\chi)$, $E_{\rm rel}(\chi)$ and $\alpha(\chi)$ correlation contours (Figs. 1, 3 and 5) show for both He and H_2 targets a dominant structure at small χ. Actually population of the K + Na^+ channels requires *electronic* excitation (Fig. 2) which does not necessarily require hard collisions with the atomic cores of the molecule and may therefore appear at rather small scattering angles [1]. For NaK^+, an $E_{\rm rel}$ value of 0.25 eV with both targets suggests a transition to the first $^2\Sigma$ (4sK) excited state dissociating into the K(4s) + Na^+ channel. This $E_{\rm rel}$ value is much smaller than that found for the dissociation resulting from the excitation of the lowest $^2\Sigma_u$ state of K_2^+ ($E_{\rm rel} = 0.6$ eV in Fig. 2) and Na_2^+ ($E_{\rm rel} = 0.8$ eV) [1,2] due to shape of the first antibonding state of the asymmetric system (Fig. 2).

Table 1. Relative probabilities for electronic (EM), impulsive (IM) and the combination of both mechanisms (IM + EM). "Scattered fragments" indicates which core is hit in the impulsive process. The values in brackets given for K_2^+ dissociation are estimates of the K(4p) excitation probabilities obtained as the difference between the contributions at $\phi = 0°$ and $\phi = 180°$ (see Fig. 6).

		Scattered fragment	EM	IM	IM + EM
NaK^+ + He, Ecm = 145 eV	Na + K^+	K^+	4	35	
		Na		50	
	Na^+ + K	K	5		5
		Na^+			1
NaK^+ + H_2, Ecm = 75 eV	Na + K^+	K^+	17	18	
		Na		52	
	Na^+ + K	K	8		4
		Na^+			1
K_2^+ + He, Ecm = 117 eV	K + K^+	K	14	56	(26)
		K^+		30	(0)
K_2^+ + H_2, Ecm = 60 eV	K + K^+	K	38	49	(36)
		K^+		13	(0)

The $\alpha(\chi)$ correlation shows at small χ, especially with the He target (Fig. 5e) two structures symmetric with respect to $\alpha = 90°$. An $\alpha(E_{\rm rel})$ analysis filtered for $\chi < 5°$, not shown here, allows to better determine the location of the structure near $\alpha = 70°$ and 110° for $E_{\rm rel} = 0.25$ eV. This behaviour due to the quasi-symmetry of the system reinforces the previous attribution of this process to the dissociation of the first $^2\Sigma$(4sK) excited state. This analysis is consistent with the previous study of Na_2^+ [2] as well as the presence of similar processes with K_2^+ (Figs. 5a,b).

In all three correlation maps of Figures 1, 3 and 5, it can be clearly noticed that contours extend with increasing χ angles. They correspond to dissociation (*e.g.* the K(4s) + Na^+ channel discussed above) induced by electronic transitions occurring in close encounters with one core. In other words, this is a combination of *both electronic and impulsive dissociation mechanisms*. Notice, for example, that in the $\alpha(\chi)$ correlation of Figure 5, the contours lines of the two structures at $\alpha = 70°$ and $\alpha = 110°$ at small χ, characteristic of electronic transitions (see above), follow at larger χ angles the two straight lines given by the impulsive model.

However the most interesting feature is provided by the long tails extending at large χ angles as seen in Figures 3c and 4d for example. They *selectively* appear in very

close encounters between the target (He or H) and the K core. This is clearly demonstrated in the three types of correlation by the comparison with the prediction of the IM model. It is suggested that this structure that extends from $\chi = 20°$ to $\chi = 40°$ in the case of a He target, is associated with the opening of a new dissociation channel giving $K(4p) + Na^+$ fragments. Its population would occur at a potential energy surface crossing located at short distance between the K core and the target. A violent encounter is necessary to reach this crossing and to feed the dissociation channel. The corresponding scattering angles: $\chi = 30°$ for K^+-He and $\chi = 50°$ for K^+-H allow to locate these crossings, if the potential is known. For K^+-He, a crossing radius of 1.9 a.u. can be estimated using the potential derived from the "combining rule" [7].

This mechanism should also be efficient for populating the $K(4p) + K^+$ in K_2^+. Although the corresponding contour plots (Figs 4a,b) are dominated by the IM in the ground state, the strong $\phi(\chi)$ asymmetry at $\phi = 0°$ and $\phi = 180°$ found with both He and H_2 targets (Figs. 1a,b) can be associated with such a mechanism. This contribution which clearly shows up in the differential cross sections for NaK^+ (Figs. 6e,f) are delineated in K_2^+ data by subtracting the contribution at $\phi = 180°$ from that at $\phi = 0°$ (Figs. 6a,b).

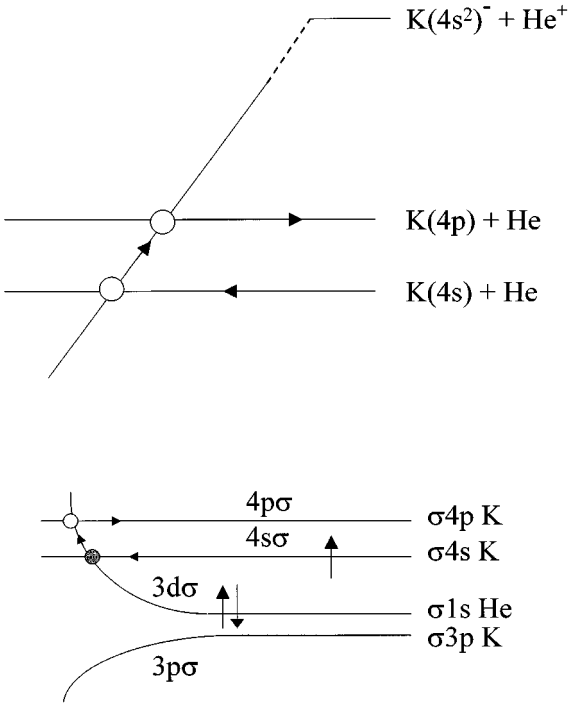

Fig. 7. Schematic diabatic molecular orbitals (bottom) and potential energy curves (top) of the K-He system in the crossing region which is suggested to account for the $K(4s) \rightarrow K(4p)$ excitation.

4 Discussion: the curve crossing mechanism

The possibility of a mechanism occurring at a potential energy surface crossing in a close encounter between two partners of the triatomic system suggests to look for a similar excitation process in the atom - atom system itself, namely in Na-He and K-He collisions. Actually, such processes have been studied in the past. Total cross sections for K(4p) and Na(3p) excitation in collisions with a He target have been measured in the keV energy range [8, 9]. Both cross sections present a similar maximum value around 2 $Å^2$ at high collision energies (few 10 keV) due to direct transitions obeying the Massey criterion [10]. But, the K(4p) cross section presents a second maximum reaching 1.6 $Å^2$ in the present $2-3$ keV energy range, while at the same energy, the Na(3p) cross section just shows a weak plateau of 0.3 $Å^2$. The similar relative importance, in our experiment, of the K and Na excitations suggests that the same type of mechanism manifests itself in the present case. In this collision energy range, the atom-atom excitation mechanism is analysed in terms of curve crossings in the corresponding diatomic quasi-molecule. This mechanism has been studied in detail for He-Na collisions [11]. It involves first the exchange interaction between the $2p_{Na}$ and 1sHe orbitals. One of the resulting molecular orbitals is promoted and interacts with the $3s_{Na}$ outer orbital thereby allowing 3p excitation through a "bridged" double crossing picture. Unfortunately similar calculations are not available for He-K, although the same type of mechanism involving the 4p electrons of the potassium ion should exist as schematically shown in Figure 7.

The role of a similar crossing for Na(3p) excitation with Na_2^+ and NaK^+ ions is not so easy to identify since the corresponding $E_{rel}(\chi)$ plots are dominated by the IM dissociation from the ground state as discussed in Section 2. Examination of the $\phi(\chi)$ contour plots could give some valuable indication as already mentioned for K_2^+. However this dissociation channel shows up neither for Na_2^+ [2] nor for NaK^+ with He target. In fact, a minimum scattering angle $\chi = 30°$ for NaK^+ is needed to reach the crossing region as estimated from the location of the crossing $R_{Na\ He} = 1.2$ a.u. given in [11] and using the ground state potential of Na^+-He of Kita *et al.* [6]. Based on this estimate, the required hard collisions are outside our experimental window ($\chi < 25°$ in this case). This channel should contribute weakly to the dissociation cross section in agreement with the results on Na^+ He collisions mentioned above [8,9]. For the NaK^+-H_2 collisions, there is no experimental limitation in χ, therefore the stretching of the contours at $\chi > 50°$ close to $\phi = 0°$ (Fig. 1f) may be attributed to the discussed mechanism.

5 Conclusions

The present study of the dissociation of NaK^+ in collisions with He and H_2 targets goes along with the previous analysis of the Na_2^+ system in terms of impulsive dissociation following a close encounter of the target with one atomic core, and of direct electronic transitions occurring in softer collisions. The relative contributions of the various dissociation channels have been determined for K_2^+ and NaK^+ ions. In particular the strong enhancement of

electronic transitions with H_2 as compared with He has been put in evidence. However investigation of an asymmetric system provides new information:

(i) The present technique allows to identify which atomic core has been hit by the target. It has enable us, in the present NaK^+ case, to evaluate the relative contribution of the K-target and Na-target encounters.

(ii) The study of the Na^++K channels allows to investigate dissociation processes requiring a combination of both basic mechanisms: a close binary encounter and an electronic transition. The kinematics of the collision allows to identify which atomic core of the molecule plays an active role in the dissociation process *via* transitions occurring at well-localised crossings. This mechanism can be analysed in terms of atom-atom transitions.

While the basic dissociation mechanisms seem now well understood for collisions with an atomic target, the situation is not as clear when considering a diatomic target. Conceptually, the impulsive mechanism involving hard core-core interactions should be better accounted for with a model based on binary collisions with a single H atom (H-model) than with a model based on collisions with H_2 considered as an atom of mass 2 (H_2-model). Comparison with experiment is not convincing. The $E_{\rm rel}(\chi)$ data are not very sensitive to the model. On the other hand, the $\alpha(\chi)$ data are in complete disagreement with the H-model.

This work has been supported by the E.U. Human Capital Mobility Program CHRX-CT-940643.

References

1. J.C. Brenot, H. Dunet, J.A. Fayeton, M. Barat, M. Winter, Phys. Rev. Lett. **77**, 1249 (1996).
2. J.A. Fayeton, M. Barat, J.C. Brenot, H. Dunet, Y.J. Picard, R. Schmidt, U. Saalmann, Phys. Rev. A **57**, 1058 (1998).
3. M. Barat, J.C. Brenot, H. Dunet, J.A. Fayeton, Z. Phys. D **40**, 323 (1997).
4. A. Valance, J. Chem. Phys. **69**, 1 (1978).
5. S. Magnier, Ph. Millié, Phys. Rev. A **54**, 204 (1996).
6. S. Kita, K. Noda, H. Inouye, J. Chem. Phys. **63**, 4930 (1963).
7. F.T. Smith, in *The Physics of Electronic and Atomic Collisions (VII ICPEAC) invited papers and progress reports*, (North Holland Eds.) pp. 1-35.
8. J.O. Olsen, N. Andersen, T. Andersen, J. Phys. B **10**, 1723 (1977).
9. N. Andersen, T. Andersen, P. Hedegaard, J.O. Olsen, J. Phys. B **12**, 3713 (1979).
10. See *e.g.* the discussion in: N. Andersen, T. Andersen, K. Bahr, C.L. Cocke, E. Horsdal Pedersen, J.O. Olsen, J. Phys. B **12**, 2529 (1979).
11. C. Courbin Gaussorgues, V. Sidis, J. Vaaben, J. Phys. B **16**, 2847 (1983).